

Optimal Energy Management for Healthcare Water Heating: Integrating Waste Heat Recovery and Solar-Assisted Heat Pumps[#]

Gaonwe T.P. ¹, Kusakana K ^{2*}, Hohne P.A. ²

¹ Department of Mechanical and Mechatronic Engineering

² Department of Electrical, Electronic and Computer Engineering
Central University of Technology, Free State
Bloemfontein, South Africa,
(kkusakana@cut.ac.za)

ABSTRACT

Healthcare facilities are among the most energy-intensive buildings, with water heating systems accounting for a significant portion of total energy consumption. Conventional electric storage tank water heaters operate inefficiently, leading to excessive energy use, frequent switching, and high peak-period demand. This study proposes an optimized energy management strategy integrating waste heat recovery and a solar-assisted heat pump to enhance system efficiency and reduce peak electricity consumption. A case study was conducted in a high-capacity healthcare facility, where baseline and optimally controlled scenarios were analyzed for both summer and winter conditions. The results indicate that the optimized control strategy successfully shifted heating loads to off-peak periods, minimized reliance on electric resistive heating, and maintained stable water temperature profiles across all tariff periods. The integration of waste heat recovery and solar-assisted heat pump significantly improved operational efficiency, demonstrating the potential for intelligent energy management solutions in large-scale healthcare water heating applications. Future work should explore real-time adaptive control mechanisms and experimental validation through pilot implementations to further enhance system adaptability and performance.

Keywords: Waste Heat Recovery, Heat Pump, Solar Energy, Energy Management, Healthcare Buildings,

NONMENCLATURE

Abbreviations

ASHP	Air-Source Heat Pump
DSM	Demand-Side Management
ESTWH	Electric Storage Tank Water Heater

ETC	Evacuated Tube Collector
GHG	Greenhouse Gas
HPHE	Heat Pipe Heat Exchanger
IPOPT	Interior Point Optimizer
MINLP	Mixed-Integer Nonlinear Programming
SAHP	Solar-Assisted Heat Pump
TES	Thermal Energy Storage
TOU	Time-of-Use
TWS	Thermal Water Storage
WHR	Waste Heat Recovery
WSHP	Water-Source Heat Pump

Symbols

abs	absorber
coll	Collector
EL	Element
hp	Heat Pump
L	Loss
S	Storage
S _{EL}	Switching / Control or Decision Variable
w	Water
wd	Water Drawn
γ	Disturbance Variable

1. INTRODUCTION

1.1 Background and Problem Statement

The building sector accounts for approximately one-third of global energy consumption, with commercial buildings, particularly healthcare facilities, being among the most energy-intensive due to continuous operation, extensive HVAC usage, and medical equipment demands (Vahidifar, Sharif, & Ghaffari, 2021). Among these energy requirements, sanitary hot water production plays a

[#] This is a paper for the Resilient-Applied Energy Symposium and Forum: Resilient energy systems (Resilient2025), Sep. 23-25, 2025, Västerås, Sweden.

critical role in hospitals, ensuring hygiene, medical sterilization, and space conditioning (Putra, Ariantara, & Manaf, 2019).

In South Africa, where electricity is the primary energy source, most hospitals rely on electric storage tank water heaters (ESTWHs) for water heating. However, these systems are highly energy-intensive, contributing to 40–50% of total electricity consumption in healthcare buildings (Dudkiewicz, Nowak, & Kwiatkowski, 2020). This dependence on electricity grids presents several challenges:

- **High Operational Costs and Peak Demand:** The morning and afternoon peak periods see a surge in electricity demand, increasing hospital energy bills and straining the national grid (Bekele, Sahle, & Teshome, 2021).
- **Environmental Impact:** Fossil fuel-based electricity use contributes to greenhouse gas (GHG) emissions, making hospitals significant carbon emitters (Sánchez-Barroso & Gutiérrez., 2020).
- **Health Risks:** Stored hot water can harbor *Legionella* bacteria, which causes Legionnaires' disease, requiring temperature control between 50°C and 60°C to prevent bacterial growth while avoiding scalding hazards (Matera & Lee, 2020).
- **Energy Security Issues:** South Africa's frequent power shortages (load shedding) threaten the reliability of hospital hot water systems, necessitating alternative solutions (Chiang, Kuo, & Lin, 2021).

Given these economic, environmental, and operational challenges, there is a critical need for energy-efficient water heating solutions that reduce costs, enhance energy security, and minimize GHG emissions in hospitals.

1.2 Need for Energy-Efficient Water Heating Solutions

Recent studies have explored multiple strategies to improve water heating efficiency in commercial and healthcare buildings, categorized into three primary approaches.

WHR captures and reuses excess heat from HVAC, chiller systems, and wastewater, reducing the need for additional heating energy (Kalina, 2020). In hospitals, WHR has been effectively applied in:

- **HVAC and Chiller Systems:** Vahidifar et al. designed a heat exchanger to recover heat from an air-cooled chiller, providing hot water for hospital laundry, resulting in significant gas savings (Fan, 2021).

- **HVAC Exhaust Air Recovery:** Putra et al. evaluated heat pipe heat exchangers (HPHEs) for hospital HVAC systems, achieving energy savings of 4.1 GJ/year (Sharma, Kumar, & V, 2021).

- **Greywater Heat Recovery:** Dudkiewicz et al. demonstrated that greywater heat exchangers could reduce hospital hot water energy demand by 30% (Chen & Wong, 2020).

WHR not only reduces energy consumption but also lowers CO₂ emissions, making it a viable approach for sustainable healthcare energy management (Wu, Luo, & Xu, 2020).

To further enhance water heating efficiency, solar thermal systems and heat pumps have been widely studied as sustainable alternatives to conventional resistance heating (Patel & Mehta, 2021).

Solar thermal collectors absorb solar radiation, providing a clean, cost-effective alternative for heating water (Johansen & Holte, 2021). Key studies include:

- Bekele et al. investigated the feasibility of solar water heating in Ethiopian hospitals, showing that solar energy could meet 81.8% of the heating load annually (Karimi & Smith, 2022).
- Sánchez-Barroso analyzed solar thermal energy systems across 25 hospitals in Spain, achieving €145,933 in annual cost savings and 637.99 tons of CO₂ reductions (Liu, Zhao, & Zhang, 2021).

Heat pumps utilize minimal electricity to transfer heat, consuming 30% less energy than conventional water heaters (Oliveira & Santos, 2022). Notable research includes:

- Matera et al. evaluated a heat pump system replacing a gas boiler in a Taiwanese hospital, cutting CO₂ emissions by 256 tons over seven months (Goyal & and Sharma, 2021).
- Chiang et al. integrated a water-source heat pump (WSHP) into an existing HVAC system, achieving \$102,564 in annual cost savings with a payback period of 1.2 years (Hassan & Khan, 2020).

Combining solar heating and heat pumps has shown even greater energy savings, particularly when integrated with thermal energy storage (TES) (Li & Sun, 2021).

Efficient energy management through thermal TES and demand-side management (DSM) can further optimize hospital energy consumption:

- **Load shifting with TES:** Storing heated water during off-peak electricity periods reduces peak-time energy costs (Tang & Liu, 2021).

- Time-of-use (TOU) pricing strategies: Adjusting heating schedules based on variable electricity tariffs has led to 20–40% cost reductions in hospitals (Wang & Zhang, 2021).

Kalina and Pohl evaluated a hospital district heating system that integrated WHR and TES, achieving CO₂ reductions of up to 2812 tons annually (Luo & Xu, 2021).

1.3 Research Gap and Objectives

C. Research Gap and Objectives

Although studies have investigated WHR, solar heating, and heat pumps individually, limited research has explored their combined integration in large-scale healthcare facilities (Cheng & Y., 2022). This study seeks to bridge this gap by developing a hybrid water heating system that integrates:

- WHR from multifunctional chillers.
- A solar-assisted heat pump (SAHP) system to enhance thermal efficiency.
- TES to improve energy savings.

The primary objectives of this research are:

- To design and evaluate a novel thermal water storage (TWS) system incorporating WHR and renewable energy technologies.
- To analyze energy efficiency, cost savings, and environmental impact in a high-capacity healthcare setting.
- To assess the economic feasibility of the proposed system compared to conventional water heating methods.

This research supports Sustainable Development Goals (SDG) 7 and 13, promoting clean energy adoption and carbon emission reduction (Sustainable Development Goals (SDGs): The 17 Goals, 2024).

2. MODEL DEVELOPMENT

2.1 System description and dynamic modelling

The proposed water heating system, as per Fig. 1, integrates a TWS tank, SAHP system, and WHR from a multifunctional chiller system. The system is designed to optimize energy efficiency by using recovered thermal energy and renewable sources to preheat water before it is supplied to a multifarious ESTWH systems.

The TWS tank is preheated using:

- Waste heat from HVAC/multifunctional chillers.
- Solar thermal energy collected by evacuated tube collectors (ETCs).
- Heat supplied by an air-source heat pump (ASHP).

Cold water enters the TWS tank, where it is preheated before being distributed to the ESTWH systems. Sensors monitor flow rates and temperatures, ensuring effective control of heating components.

To simplify the system’s mathematical modeling, the following assumptions are made:

- Uniform temperature distribution within the TWS tank.
- Fixed power rating for the heat pump during operation.
- Negligible energy losses during heat exchange.
- Steady fluid flow, with minimal changes in flow rate.

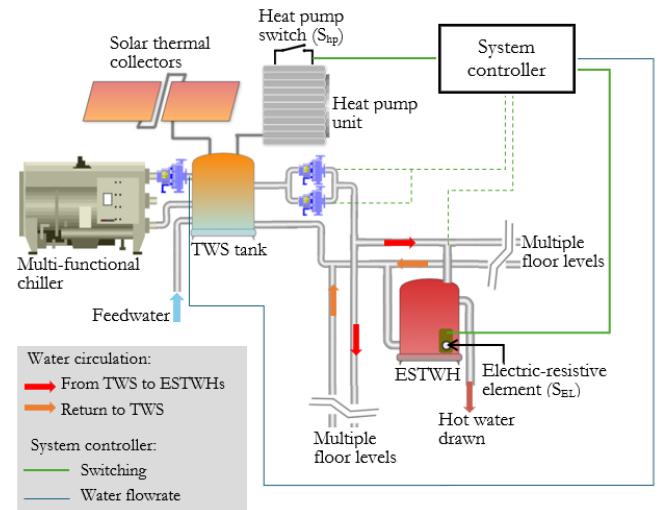


Fig. 1 Proposed system

2.2 Mathematical Model of the Proposed System

The system is modelled using energy balance equations for both the TWS tank and the ESTWH systems.

2.2.1 Energy Balance for the Thermal Water Storage (TWS) Tank

The heat energy in the TWS tank is governed by:

$$\dot{Q}_{TWS}(t) = \dot{Q}_{SAHP}(t) - \dot{Q}_{wd}(t) - \dot{Q}_{LossTWS}(t) \quad (1)$$

Where: $\dot{Q}_{TWS}(t)$ is the total thermal heating energy in the TWS tank; $\dot{Q}_{SAHP}(t)$ is the energy gain due to the thermal heat transfer from the retrofitted SAHP system; $\dot{Q}_{wd}(t)$ is the energy losses by the water drawn from the TWS tank to the ESTWHs and $\dot{Q}_{LossTWS}(t)$ is the standby heat losses of the TWS tank.

The heat input from the SAHP system includes:

$$\dot{Q}_{SAHP}(t) = \dot{W}_{hp}(t) + \dot{Q}_{coll}(t) \quad (2)$$

The heat pump's contribution is modelled as:

$$\dot{W}_{hp}(t) = COP \times P_{hp} t_{(h)} S_{hp}(t) \quad (3)$$

Where: $P_{hp}(t)$ is the input power to the HP (kW); $t_{(h)}$ is time of operation (hour) and $S_{hp}(t)$ is the control switch of the HP.

The energy gain by the solar system when sunlight is available (particularly during the day) is determined using the given in Eq. (4) (Chiang, Kuo, & Lin, 2021):

$$\dot{Q}_{coll}(t) = \eta \times I_{\beta}(t) A_{abs} t_{(h)} \quad (4)$$

Where: η is the tube efficiency of the collector; $I_{\beta}(t)$ is the Solar irradiance (W/m^2); and A_{abs} is the absorber area of the collector

The hot water drawn from the TWS tank to the ESTWHs ($\dot{Q}_{wd}(t)$) occur as a makeup water when water is drawn from the ESTWHs by the end users and is given as follows:

$$\dot{Q}_{wd}(t) = \dot{m}_{TWS}(t) C_{p,w} [T_{TWS}(t) - T_{pre}(t)] \quad (5)$$

Where: $\dot{m}_{TWS}(t)$ is the flow rate of the water drawn from the TWS tank (kg/s) and $T_{pre}(t)$ is the temperature of the preheated water by the heat recovered from the Multifunctional chillers.

The standby losses, $\dot{Q}_{LossTWS}(t)$, denote power losses resulting from the surface conduction of the casing material and is given as in Eq. (6):

$$\dot{Q}_{LossTWS}(t) = U_{TWS} t_{(h)} A_{TWS} [T_{TWS}(t) - T_{amb}(t)] \quad (6)$$

Where: U_{TWS} is the coefficient of the heat loss of the TWS tank in ($W/m^2 \text{ } ^\circ C$) and A_{TWS} is the surface area of the TWS tank (m^2).

By substituting Eqs. (2), (5) and (6) into (1), and after simplification, the state space equation can be derived. This equation has three variables which are the state variable ($\dot{T}_{TWS}(t)$), the control or decision variables ($S_{hp}(t)$) and the disturbance variable in the system ($\gamma_{TWS}(t)$) and the expression is given in Eq. (7):

$$\dot{T}_{TWS}(t) = -A_{TWS}(t) T_{TWS}(t) + B_{TWS} S_{hp}(t) + \gamma_{TWS}(t) \quad (7)$$

2.2.2 Energy Balance for the ESTWH system

The open energy balance for the ESTWH system is expressed as the thermal energy gain from the electric resistive element ($\dot{Q}_{EL}(t)$) and the energy losses due to hot water demand ($\dot{Q}_D(t)$) and standby losses ($\dot{Q}_L(t)$). The resulting energy balance ($\dot{Q}_{ESTWH}(t)$) equation, with the heat gains and losses in the system, is given in Eq.:

$$\dot{Q}_{ESTWH}(t) = \dot{Q}_{EL}(t) - \dot{Q}_L(t) - \dot{Q}_D(t) \quad (8)$$

The energy balance ($\dot{Q}_{ESTWH}(t)$), expressed as a first derivative differential function, representing the heat energy in the ESTWH equates to the following:

$$\dot{Q}_{ESTWH}(t) = M_w C_{p,w} \dot{T}_S(t) \quad (9)$$

Where: M_w is the mass of water inside the storage tank (kg) and $\dot{T}_S(t)$ is the variable temperature of the water inside the ESTWH system ($^\circ C$).

The electric resistive element serves as a backup power source (P_{EL}) to enhance hot water availability in the event of low thermal energy from the SAHP system. Therefore, electrical energy ($\dot{Q}_{EL}(t)$) will be supplied to the electric resistive element, which is controlled by the switch ($S_{EL}(t)$), to sustain the desired temperature, as presented:

$$\dot{Q}_{EL}(t) = P_{EL} t_{(h)} S_{EL}(t) \quad (10)$$

In a baseline case, the heat losses in the ESTWH are caused by the makeup water which enters at a low temperature whenever there is hot water demand draw-offs occurring. As a result, there is temperature decrease inside the ESTWH system when cold water flows into the tank to maintain a consistent volume. However, in this case the makeup water mostly, if not always, enters at a temperature equal or slightly higher than the maximum desired (set) temperature. The thermal energy losses of the hot water demand $\dot{Q}_D(t)$ is, therefore, given in Eq. (11).

$$\dot{Q}_D(t) = \dot{W}_D(t) C_{p,w} [T_{TWS}(t) - T_S(t)] \quad (11)$$

Where: \dot{W}_D is the variable hot water demand mass flow rate (kg/h).

The other losses in the ESTWH is standby losses, $\dot{Q}_L(t)$, for the ESTWH given as in Eq. (12):

$$\dot{Q}_L(t) = U_S t_{(h)} A_S [T_S(t) - T_{amb}(t)] \quad (12)$$

By substituting all variables and coefficients (parameters) from Eqs. (9) – (12), into the energy balance, Eq. (8), and after simplification, the state space equation can be derived as Eq. (13), the variables are the state variable ($\hat{T}_s(t)$), the control or decision variable is ($S_{EL}(t)$) and the disturbance variable in the ESTWH system is ($\gamma_s(t)$):

$$\hat{T}_s(t) = -A_s(t)T_s(t) + B_s S_{EL}(t) + \gamma_s(t) \quad (13)$$

2.2.3 Discretized hot water temperature

The state space equation may be created, using the energy balance equation. To show how the temperature of the water inside the storage tank changes, the continuous temperature function (\hat{T}_k) is converted into a generic discrete formulation, yielding Eq. (14):

$$\begin{aligned} \hat{T}_{(z),k+1} = T_{(z),0} & \prod_{j=0}^k (1 - t_s A_{(z),j}) \\ & + t_s B_{(z)} \sum_{j=0}^k S_{(y),j} \prod_{i=j+1}^k (1 \\ & - t_s A_{(z),i}) \\ & + t_s \sum_{j=0}^k \gamma_{(z)} \prod_{i=j+1}^k (1 \\ & - t_s A_{(z),i}) \end{aligned} \quad (14)$$

Where: z indicates either the TWS tank or ESTWH system and y indicates the switching of either the HP unit or the electric resistive element, respectively.

2.3 Optimization Control Problem

2.3.1 Objective function

The aggregate objective function for the heat pump unit and the electric resistive elements becomes Eqs. (15) and (16):

- TWS tank

$$\begin{aligned} \min J_{TWS,t} = t_s \sum_{k=1}^N (P_{hp,k} S_{hp,k}) \times p_k + \\ t_s \times p_{k,MAX} \sum_{k=1}^N (P_{hp,k} S_{hp,k}) \end{aligned} \quad (15)$$

- ESTWH system

$$\begin{aligned} \min J_{S,t} = t_s \left(\sum_{k=1}^N P_{EL(1),k} S_{EL(2),k} \times p_k \right. \\ \left. + \sum_{k=1}^N P_{EL(1),k} S_{EL(2),k} \times p_k \right. \\ \left. + \dots \right. \\ \left. + \sum_{k=1}^N P_{EL(N),k} S_{EL(N),k} \times p_k \right) \quad (16) \\ + t_s \\ \times p_{k,MAX} \sum_{k=1}^N (P_{EL(1),k} S_{EL(2),k} \\ + P_{EL(1),k} S_{EL(2),k} + \dots \\ + P_{EL(N),k} S_{EL(N),k}) \end{aligned}$$

The objective function, shown in Eqs. (15) and (16), is a non-linear mixed integer function with a binary control variable that should be solved in order to obtain the optimal switching status function of the heat pump compressor switch and the electric resistive element.

2.3.2 Constraints on Temperature and Switching States

The objective functions are subject to the following constraints:

$$\begin{aligned} T_k^{\min} \leq T_{(z),0} & \prod_{j=0}^k (1 - t_s A_{(z),j}) \\ & + t_s B_{(z)} \sum_{j=0}^k S_{(z),j} \prod_{i=j+1}^k (1 \\ & - t_s A_{(z),i}) \\ & + t_s \sum_{j=0}^k \gamma_{(z)} \prod_{i=j+1}^k (1 \\ & - t_s A_{(z),i}) \end{aligned} \quad (17)$$

$$\begin{aligned} T_{(z),0} & \prod_{j=0}^k (1 - t_s A_{(z),j}) \\ & + t_s B_{(z)} \sum_{j=0}^k S_{(z),j} \prod_{i=j+1}^k (1 \\ & - t_s A_{(z),i}) \\ & + t_s \sum_{j=0}^k \gamma_{(z)} \prod_{i=j+1}^k (1 \\ & - t_s A_{(z),i}) \leq T_k^{\max} \end{aligned} \quad (18)$$

Where z represents either the TWS tank or ESTWH system; T_k^{\min} is the minimum permissible temperature for the hot water inside the TWS tank and ESTWH system; and T_k^{\max} is the maximum threshold that the temperature may not exceed, for any given interval.

2.3.3 Optimization Solver

The optimization problem is formulated as a Mixed-Integer Nonlinear Programming (MINLP) problem and

solved using the SCIP solver in MATLAB. The Interior Point Optimizer (IPOPT) is used to handle nonlinear constraints

3. SIMULATION RESULTS AND DISCUSSION

The case study for this project is one of the high-capacity healthcare facilities in the Bloemfontein, Free State. The facility has a total of 12 theatres, 383 beds (75 ICU beds) with an additional 22 beds in the process of admission for medical reasons. The main building has a combined floor size of approximately 10,500 m². The water heating network of the hospital consists of 57 ESTWH systems, supplied with pre-heated water from a waste heat recovery system.

The hot water demand profiles for the summer and winter seasons are presented in Fig. 2 and Fig. 3, showing the hot water demand profiles of the multifarious ESTWH systems in 24 hours.

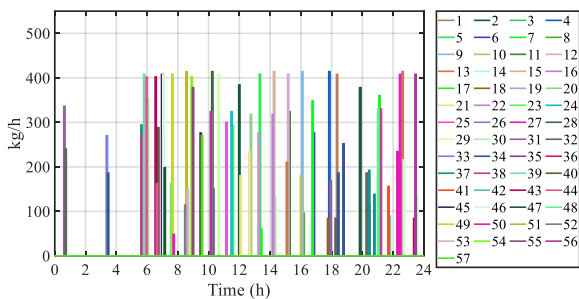


Fig. 3 Hot water demands from multifarious ESTWH systems during summer season

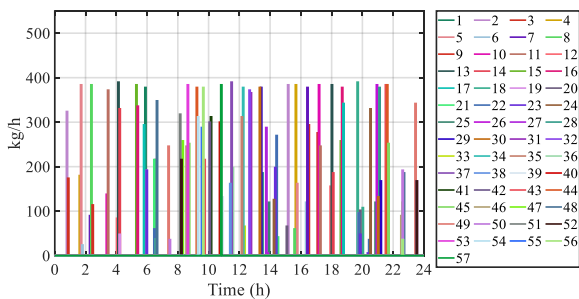


Fig. 2 Hot water demands from multifarious ESTWH systems during winter season

3.1 Baseline

3.1.1 Baseline switching profiles and water temperatures: summer season

This section evaluates the baseline switching profiles (Fig. 4) and water temperature variations of the ESTWH

systems (Fig. 5) during the summer season, focusing on their operational behavior under a TOU tariff structure.

Throughout the off-peak period (00h00 – 06h00), minimal switching is observed as the system maintains water temperatures, although some ESTWH units experience a gradual temperature decline below 50°C. During the standard period (06h00 – 07h00), switching activity increases as temperatures continue to drop, leading to heightened activation of heating elements. The peak period (07h00 – 10h00) witnesses significant switching activity due to a marked drop in water temperatures necessitating recovery. The subsequent standard period (10h00 – 18h00) maintains a relatively consistent switching pattern, primarily sustaining water temperatures with minimal recovery events. In the evening peak period (18h00 – 20h00), switching intensifies again, as water temperatures fall below 50°C in many systems. The late standard period (20h00 – 22h00) and off-peak period (22h00 – 24h00) show sustained switching activity, ensuring water temperature stability.

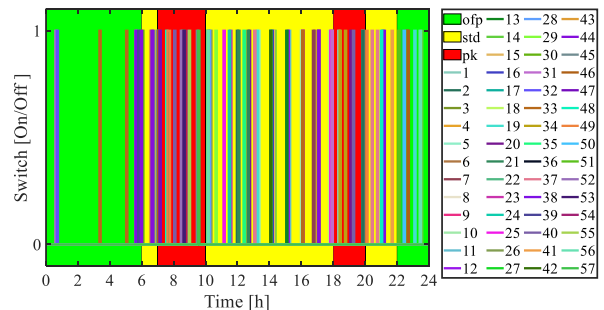


Fig. 4 Baseline switching function for Multifarious ESTWH systems during summer season

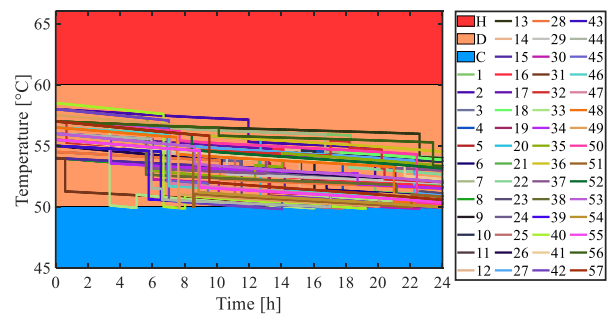


Fig. 5 Baseline storage tank temperatures for Multifarious ESTWH systems during summer season

3.1.2 Baseline switching profiles and water temperatures: winter season

This section extends this analysis to the winter season, where baseline ESTWH switching profiles (Fig. 6) and temperature (Fig. 7) variations are evaluated under colder conditions.

Unlike in summer, switching activity during the off-peak period (00h00 – 06h00) is more frequent to elevate water temperatures above 55°C across all floors. The morning peak period (06h00 – 09h00) exhibits sustained switching as temperatures drop, with some instances of water falling below 50°C. During the standard period (09h00 – 17h00), water temperatures steadily decline, requiring continued switching to restore them above 50°C. The evening peak period (17h00 – 19h00) again sees intensified switching due to significant temperature drops. The late standard period (19h00 – 22h00) follows a similar trend, with temperature fluctuations necessitating frequent switching interventions. Finally, in the off-peak period (22h00 – 24h00), water temperatures stabilize slightly, but switching remains necessary to maintain the required threshold. The winter season presents a more energy-intensive scenario due to increased heating demands, leading to prolonged operational hours of the ESTWH systems and a corresponding rise in electricity consumption.

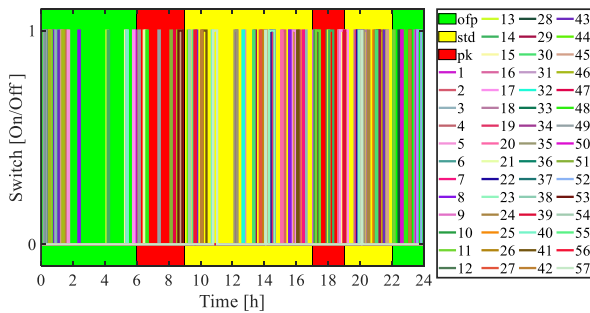


Fig. 6 Baseline switching function for Multifarious ESTWH systems during winter season

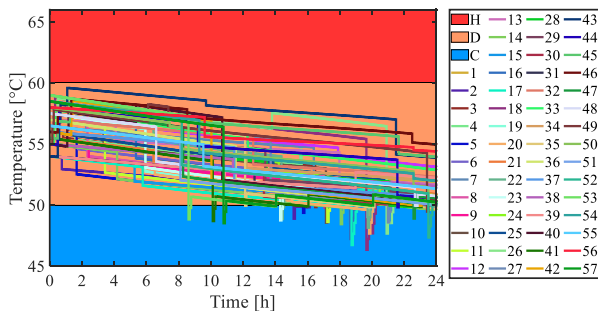


Fig. 7 Baseline storage tank temperatures for Multifarious ESTWH systems during summer season

3.2 System performance: optimally controlled cases

3.2.1 Optimally controlled switching profiles and water temperatures: Summer season

This section analyzes the optimally controlled switching profiles (Fig. 8) and water temperatures (Fig. 9) for the summer season, demonstrating the impact of an advanced DSM strategy. The retrofitted SAHP system supplements the TWS tank, allowing for more efficient heating patterns.

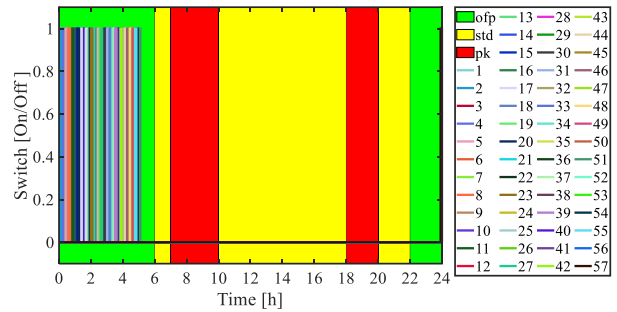


Fig. 8 Optimal switching function for Multifarious ESTWH systems during summer season

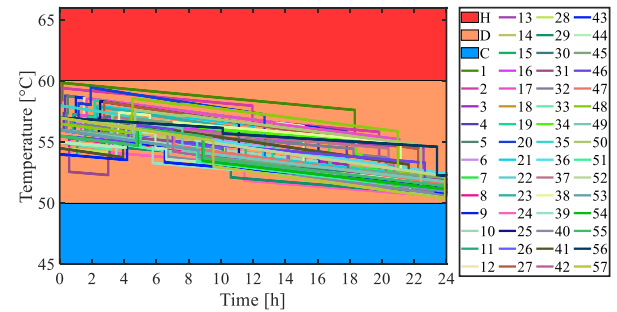


Fig. 9 Optimal storage tank temperatures for Multifarious ESTWH systems during summer season

During the off-peak period (00h00 – 06h00), the heat pump remains inactive, and the TWS tank temperature declines slightly from 56°C to 55°C, while the majority of switching in the multifarious ESTWH systems shifts to this period, resulting in a widespread temperature increase across all floor levels. In the subsequent standard period (06h00 – 07h00), no switching occurs in either the heat pump or the ESTWH systems, causing water temperatures to decrease gradually, though remaining above 50°C. Throughout the morning peak period (07h00 – 10h00), no switching occurs, and the TWS tank temperature continues to drop slightly before recovering due to solar thermal energy input. The midday standard period (10h00 – 18h00) sees a continuous temperature rise in the TWS tank, exceeding

60°C by the evening, while no switching is needed in the ESTWH systems, ensuring steady water temperature levels. This optimized control strategy significantly reduces peak-period electricity demand, shifting heating loads to off-peak hours, improving energy efficiency, and minimizing operational costs.

3.2.2 *Optimally controlled switching profiles and water temperatures: Winter season*

This section evaluates the optimally controlled switching profiles (Fig. 10) and water temperature dynamics (Fig. 11) for the winter season, demonstrating the impact of integrating a SAHP system and DSM strategies. Unlike in summer, the SAHP operates strategically to maintain water temperature levels, beginning with an early morning activation that slightly increases the TWS tank temperature.

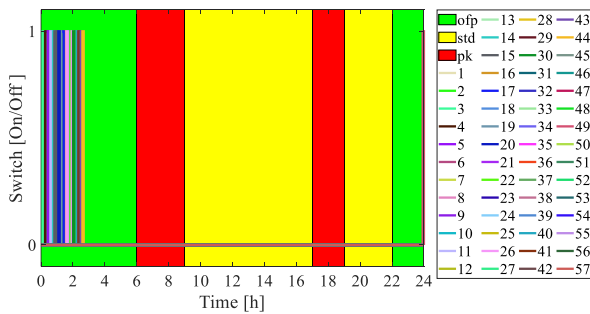


Fig. 10 Optimal switching function for Multifarious ESTWH systems during winter season

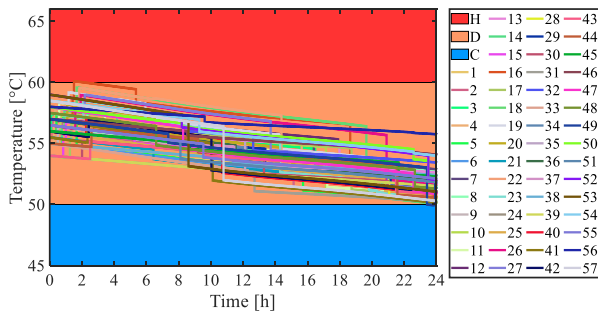


Fig. 11 Optimal storage tank temperatures for Multifarious ESTWH systems during winter season

Throughout the morning peak period (06h00 – 09h00), no switching occurs in the heat pump, resulting in a minor temperature decline of approximately 5°C. During the standard period (09h00 – 17h00), temperatures within the TWS tank stabilize with minimal fluctuations due to solar thermal input. In the evening peak period (17h00 – 19h00), the absence of switching

causes a gradual temperature decrease, which continues into the standard period (19h00 – 22h00). Finally, during the off-peak period (22h00 – 24h00), the heat pump resumes operation, restoring the TWS tank temperature to 55°C, ensuring a stable supply of preheated water to the ESTWH systems. The optimized control significantly reduces peak-period energy demand by shifting heating loads to off-peak hours, mitigating the reliance on electric resistive elements, and enhancing overall system efficiency.

3.3 *Comparison between the baseline and optimally controlled systems*

From the above, the power consumption of the multifarious ESTWH systems, comparing baseline and optimally controlled cases for both summer and winter seasons. In the summer scenario, the baseline case exhibits continuous power consumption throughout the day, with a significant demand spike during the evening peak period. The optimally controlled system shifts heating loads to the early morning off-peak hours and the last hour of the day, thereby reducing electricity demand during peak tariff periods. Notably, the optimal system shows no power consumption for the heat pump unit, indicating a reliance on solar thermal energy to sustain heating. For the winter season, the baseline system again demonstrates continuous power usage, but the highest demand occurs during the early morning off-peak period. In contrast, the optimally controlled system strategically shifts power consumption to off-peak periods, with the heat pump unit operating during the morning and evening off-peak hours. The findings underscore the effectiveness of the optimal control strategy in reducing peak-period power consumption, improving overall energy efficiency, and minimizing operational costs

4. CONCLUSIONS

This study has presented an optimized energy management strategy for a large-scale healthcare facility, integrating WHR and a SAHP to improve the efficiency of multifarious ESTWH systems. The baseline analysis revealed that conventional ESTWH systems exhibit frequent and uncoordinated switching, leading to unnecessary peak-period energy consumption and inefficiencies in water heating. The implementation of an optimal control strategy successfully shifted heating loads to off-peak periods, reducing high-demand electricity usage while maintaining the required water

temperature levels. The integration of WHR and SAHP provided a stable preheated water supply, minimizing the reliance on electric resistive heating elements.

The optimized system demonstrated significant improvements in operational performance, particularly in reducing peak-period switching and stabilizing temperature profiles across different tariff periods. In both summer and winter conditions, the proposed strategy effectively leveraged renewable energy and waste heat, reducing overall energy demand while ensuring consistent hot water availability. The findings underscore the potential of intelligent energy management solutions in mitigating inefficiencies in large-scale healthcare water heating systems.

ACKNOWLEDGEMENT

This work is based on the research supported wholly / in part by the National Research Foundation of South Africa (Grant Numbers: RCHDI241020275598)

REFERENCES

(2024, December 10). Retrieved from Sustainable Development Goals (SDGs): The 17 Goals: <https://sdgs.un.org/>

Bekele, G., Sahle, A., & Teshome, B. (2021). Feasibility of Solar Water Heating in Ethiopian Hospitals. *Sustainable Energy Technologies and Assessments*, 42.

Chen, Z., & Wong, K. K. (2020). Economic and Environmental Analysis of Solar Water Heating in Large-Scale Healthcare Facilities. *Applied Energy*, 272.

Cheng, L., & Y., D. (2022). Evaluating the Performance of Hybrid Heat Pump-Solar Water Heating Systems in Large Healthcare Facilities. *Energy Reports*, 8, 455–466.

Chiang, H., Kuo, J. M., & Lin, W. S. (2021). Integration of Water-Source Heat Pumps in Hospital HVAC Systems: Cost and Energy Efficiency Analysis. *Journal of Building Engineering*.

Dudkiewicz, E., Nowak, A., & Kwiatkowski, P. (2020). Greywater Heat Recovery in Hospitals: A Case Study. *Renewable Energy*, 147, 2454–24.

Fan, X. a. (2021). Impact of Thermal Energy Storage on Load Shifting in Hospitals. *Journal of Energy Storage*, 36.

Goyal, A., & and Sharma, P. (2021). Smart Grid Solutions for Hospital Water Heating Systems: Demand Response Strategies. *International Journal of Energy Research*, 45(12), 1784–1797.

Hassan, R., & khan, A. (2020). The Role of Thermal Storage in Hospital Water Heating: A Case Study in South Africa. *Energy Procedia*, 156, 789–794.

Johansen, B., & Holte, L. (2021). Load Forecasting for Smart Hospital Energy Systems. *Energy Reports*, 7, 1235–1245.

Kalina, J. a. (2020). District Heating Systems in Healthcare Facilities: Integration of Waste Heat Recovery and Thermal Storage. *Energy and Buildings*, 209.

Karimi, A., & Smith, J. C. (2022). Application of AI in Hospital Energy Management: A Case Study on Water Heating Optimization. *Journal of Building Performance*, 2022): 88–97.(1), 88–97.

Li, H., & Sun, X. (2021). Performance Analysis of a Solar-Assisted Heat Pump for Water Heating in Hospitals. *Applied Thermal Engineering*, 198, 117495.

Liu, W., Zhao, Z., & Zhang, P. (2021). An Intelligent Control System for Optimizing Water Heating in Healthcare Facilities. *Energy Science & Engineering*, 9(4), 712–725.

Luo, X., & Xu, P. (2021). Economic Feasibility of Integrating Waste Heat Recovery with Solar Water Heating in Hospitals . *Sustainable Energy Technologies and Assessments*, 47, 101391.

Matera, C., & Lee, T. (2020). Heat Pump System as a Replacement for Gas Boilers in Hospitals: Energy and Emission Reductions. *Energy Reports* , 318–327.

Oliveira, T., & Santos, F. (2022). Hybrid Renewable Energy Systems in Healthcare Facilities: A Review of Water Heating Strategies. *Renewable Energy*, 182, 405–418.

Patel, R., & Mehta, A. (2021). Efficiency Evaluation of Heat Pump Water Heating in Hospitals. *Energy Efficiency*, 14(2).

Putra, N., Ariantara, D., & Manaf, A. (2019). Waste Heat Recovery from Hospital HVAC System Using Heat Pipe Heat Exchanger. *Applied Thermal Engineering*, 160.

Sánchez-Barroso, G., & Gutiérrez., L. (2020). Solar Thermal Energy in Hospitals: Energy Savings and Environmental Impact. *Renewable and Sustainable Energy Reviews*, 133.

Sharma, R., Kumar, M., & V, S. (2021). A Review of Time-of-Use Pricing Strategies in Hospital Energy Management. *Renewable and Sustainable Energy Reviews*, 152.

Tang, Y., & Liu, J. (2021). Heat Recovery from Hospital Laundry for Sustainable Water Heating. *Journal of Environmental Management*, 286, 112200.

Vahidifar, S., Sharif, M. N., & Ghaffari, M. (2021). Heat Recovery System from Air-Cooled Chillers in Iranian Hospitals. *International Journal of Civil and Architectural Engineering*, 15(1).

Wang, J., & Zhang, R. (2021). AI-Driven Optimization of Water Heating Load Distribution in Healthcare Facilities. *Energy and AI*, 5, 100091.

Wu, H., Luo, X., & Xu, P. (2020). Optimization of Waste Heat Utilization in Hospital Heating System. *Energy and Buildings*, 206.